Shan Yong
Jiangsu Province Key Laboratory
of Aerospace Power System,
College of Energy and Power Engineering,
Nanjing University of Aeronautics
and Astronautics,
29 Yudao Street,
Nanjing 210016, China
e-mail: nuaasy@nuaa.edu.cn

Zhang JingZhou[1]
Jiangsu Province Key Laboratory
of Aerospace Power System,
College of Energy and Power Engineering,
Nanjing University of Aeronautics
and Astronautics,
29 Yudao Street,
Nanjing 210016, China
e-mail: zhangjz@nuaa.edu.cn

Wang Yameng
Jiangsu Province Key Laboratory
of Aerospace Power System,
College of Energy and Power Engineering,
Nanjing University of Aeronautics
and Astronautics,
29 Yudao Street,
Nanjing 210016, China
e-mail: 13915973855@139.com

Numerical Investigation on Aerodynamic and Combustion Performance of Chevron Mixer Inside an Afterburner

To improve the performance of the afterburner for the turbofan engine, an innovative type of mixer, namely, the chevron mixer, was considered to enhance the mixture between the core flow and the bypass flow. Computational fluid dynamics (CFD) simulations investigated the aerodynamic performances and combustion characteristics of the chevron mixer inside a typical afterburner. Three types of mixer, namely, CC (chevrons tilted into core flow), CB (chevrons tilted into bypass flow), and CA (chevrons tilted into core flow and bypass flow alternately), respectively, were studied on the aerodynamic performances of mixing process. The chevrons arrangement has significant effect on the mixing characteristics and the CA mode seems to be advantageous for the generation of the stronger streamwise vortices with lower aerodynamic loss. Further investigations on combustion characteristics for CA mode were performed. Calculation results reveal that the local temperature distribution at the leading edge section of flame holder is improved under the action of streamwise vortices shedding from chevron mixers. Consequently, the combustion efficiency increased by 3.5% compared with confluent mixer under the same fuel supply scheme. [DOI: 10.1115/1.4027604]

1 Introduction

The aircraft engine afterburner is an extension to a turbine engine that provides the additional thrust for take-off from short runways, rapid acceleration, and supersonic flight. The afterburner increases thrust by burning additional fuel in the turbine exhaust stream. It is known that the mixer employed in turbofan engine afterburners is of significant importance on the mixing process between core flow and bypass flow (or fan flow). It has some effect on the combustion efficiency, too. As a common mixer, confluent mixer has been widely used in the afterburner for its simple structure and less mixing aerodynamic loss. However, the confluent mixer leads core flow and bypass flow to mix in a shear diffusion manner with a lower mixing efficiency. It may lead to unsatisfactory oxygen and temperature distributions in the front of the flame holder. It results in lower combustion efficiency of afterburner combustor. Concerning the forced mixer or lobed mixer, it has been proven to a kind of mixers with higher mixing efficiency, for the reason is that the streamwise vortex induced by the lobe mixer forces the two parallel flows to mix in a convective manner. Investigations on various types of lobed mixers have been adequately documented [1–9]. The lobe mixer periodically converts the spanwise vortices into streamwise vortices and increases the interfacial area. It is the key contributors to the mixing enhancement. A convoluted mixer has relatively shallow penetration ability, which expects to generate only weak streamwise vortices. An angle mixer, on the other hand, is the simplest possible form that directs the annular flow into the core forcing its diffusion in the core flow; however, the forced deflection of the completely annular flow results in a significant total pressure loss. It is common practice to consider both pressure loss and mixing efficiency as contradicting parameters, the synergy of aerodynamic loss and mixing efficiency is a key issue for the optimum design of mixer. In the current study, an innovative type of mixer, that is chevron mixer, was presented in afterburner of turbofan engine with low bypass. Up to now, there appears to be no literature dealing with the application of chevron mixers in a low bypass turbofan afterburner.

It has been known for a long time that tabs, small protrusions placed near the nozzle exit, enhance mixing in two confined, co-axial jets. In the 1980s and 1990s, the tabs were explored extensively for mixing enhancement in jets [10–12]. These studies advanced the understanding of the flow mechanisms and suggested that the technique has a potential performance for reduction of turbulent mixing noise that is the dominant component of jet noise for most aircraft. The chevron nozzle is originated from tabbed nozzle, employing serrations on the nozzle trailing edge, which represents the current state in jet noise reduction technology for application in medium and high bypass turbofan engines. Chevrons are extensions of the nozzle wall into a continuous serrated edge. In contrast, the tabs are to have "hard breaks" and more aggressive penetration into the flow, shown in Fig. 1.

The chevron nozzles shown in Fig. 2 possess triangular serrations along the trailing edge, which induce streamwise vorticity into the shear layer. This results in enhanced mixing and reduced jet plume length. According to Bridges and Brown [13], the chevron count controls the azimuthal spacing between the axial vortices, whereas chevron penetration controls the strength of the axial vortices and chevron length controls the distribution of vorticity within axial vortices. Callender et al. [14,15] experimentally investigated single and dual flows for baseline inner nozzle and three chevron nozzles over a wide range of operating conditions. Chevrons with varying numbers of lobes and levels of penetration were studied to understand the impact of these geometric parameters on far-field acoustics. Spectral and directivity results from heated co-axial jets showed that the chevron nozzles were most effective at lower frequencies and at aft directivity angles. Opalski

[1]Corresponding author.

Contributed by the Combustion and Fuels Committee of ASME for publication in the Journal of Engineering for Gas Turbines and Power. Manuscript received December 31, 2013; final manuscript received April 3, 2014; published online May 16, 2014. Assoc. Editor: Klaus Dobbeling.

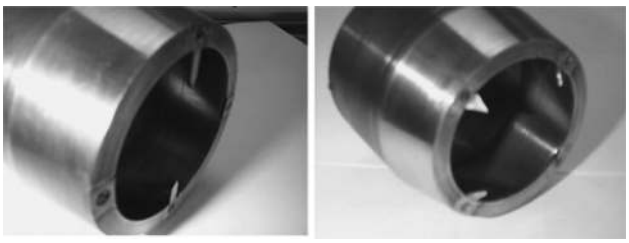

Fig. 1 Tabs on the nozzle outlet (Ref. [16])

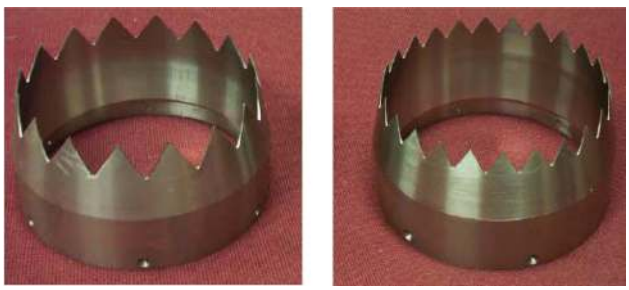

Fig. 2 Chevron nozzles (Ref. [17])

et al. [18] used stereoscopic digital particle image velocimetry to characterize the flow fields from chevron nozzles and a baseline circular nozzle. Nozzle outlet conditions ranged from Mach numbers of 0.9–1.5. Three-dimensional features of the turbulent jet evolution were captured. They measured and reported well-defined streamwise vortex structures in the jet shear layers. Furthermore, examination of the relationships between chevron geometric parameters and flow characteristics was performed. Tide and Srinivasan [19] proposed two novel chevron concepts and evaluates their noise reduction performance. The new chevron concepts proposed were protrusions with a sinusoidal profile and chevrons with asymmetry. These nozzles were compared against the symmetric chevron nozzle with triangular profile and a baseline circular nozzle without chevrons. The results indicated that the sinusoidal profile chevron nozzle shows better noise reduction at higher-pressure ratios for all emission angles. Zaman et al. [20] presented a review of evolution from tabs to chevron technology.

The concept of chevron mixer in the current study is originated from chevron or tabbed nozzle. It is expected to be applied inside afterburner to produce desirable mixing of the cold bypass and flow and the hot core flow prior to their flow through the flameholder with minimum pressure loss. Although the potential of chevron nozzle for noise suppressing application was realized in the last decade, no studies have performed on the chevron mixer involving afterburner. A justifiable need for undertaking a systematic investigation on mixing and combustion performances is a help for a chevron mixer configuration, pertinent to a low bypass aircraft engine. The motivation of the present work is to outline the aerodynamic performances and combustion characteristics of chevron mixer inside a typical afterburner by using CFD simulations. First, nonreacting flow fields were simulated for three kinds of chevron mixers (e.g., chevrons tilted into core flow, chevrons tilted into bypass flow, and chevrons tilted into core flow and bypass flow alternately) to analyze the aerodynamic performances of mixing process. Then a typical chevron mixer was chosen to compare the combustion characteristics relative to confluent mixer qualitatively.

1.1 Physical Model. A simplified afterburner model considered in the current study is schematically shown in Fig. 3. It consists mainly of inlet struts, mixer, flameholder, central cone, and augmentor. Hot vitiated core flow from low-pressure turbine

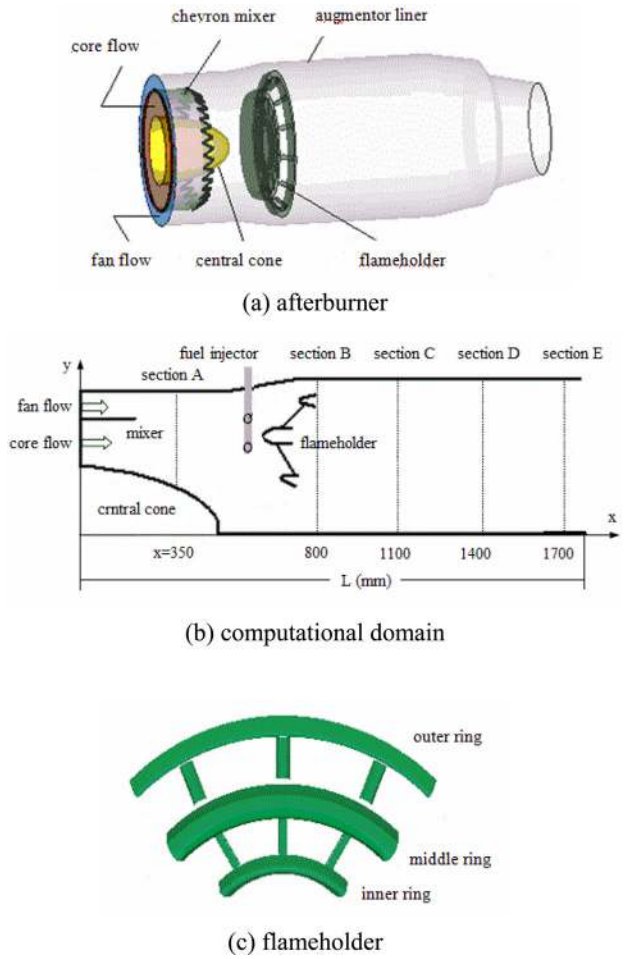

Fig. 3 Schematic of simplified afterburner model: (*a*) afterburner, (*b*) computational domain, and (*c*) flameholder

enters the annulus of the exhaust diffuser having nine twisted struts at the inlet. Cold air is driven by the fan to enter through the bypass duct and mix with the core flow through mixer. Fuel is introduced into the augmentor using a series of radial struts with a large number of fuel injection sites. The flame is typically stabilized using an array of bluff-body flameholders, which are made of V-shaped gutters providing robust fluid recirculation zones in the flow to anchor the flame in space within the augmentor cavity. The fuel injector is fixed at the upstream of the flameholder with 135 nozzles (each of 0.4 mm in diameter) around the circumference. The coordinate origin is located at the inlet of afterburner. The diameter of the combustion chamber is 1.0 m and the length is 1.8 m. Five sections are specialized in Fig. 1, they are marked as A, B, C, D and E, respectively.

Chevrons are saw tooth-like patterns at the trailing edge of confluent mixer, as seen in Fig. 4. According to the arrangement of chevrons, three kinds of chevron mixers were designed, they are denoted as CC (chevrons tilted into core flow), CB (chevrons tilted into bypass flow), and CA (chevrons tilted into core flow and bypass flow alternately), respectively. The confluent mixer is a baseline mixer, named as CM. All the chevron mixers have the same chevrons ($n = 30$) and chevron length ($S/D = 0.18$, where D is mixer diameter). The chevron penetration angle is set in Table 1.

1.2 Numerical Model

(1) Nonreacting flowfield
The nonreacting flow in afterburner was assumed as steady, 3D, and turbulent. The flow is governed by the conservation

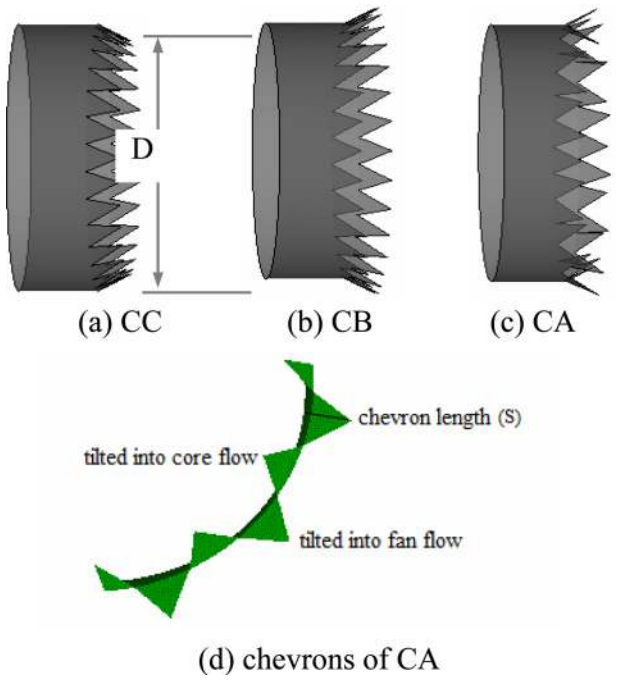

Fig. 4 Schematic of chevrons: (*a*) CC, (*b*) CB, (*c*) CA, and (*d*) chevrons of CA

equations of mass, momentum, and energy, turbulent kinetic energy and its dissipation rate. The general form of these conservation equations can be written as follows:

$$\frac{\partial}{\partial t}(\rho\varphi) + \mathrm{div}(\rho\vec{V}\varphi) = \mathrm{div}(\Gamma^{\varphi}\mathrm{grad}\varphi) + S^{\varphi} \quad (1)$$

where φ represents the dependent variable (stands for velocity components u, v, and w, temperature T, turbulent kinetic energy k, and dissipation rate ε), Γ^{φ} is the effective diffusion coefficient of variable φ and S^{φ} is the source term for the equation.

In the present computation, renormalization group k–ε turbulence model with wall function approach is used to simulate turbulence. The turbulence model has been validated in some articles [21,22] with experimental and numerical results. It is a good choice to present the development of the streamwise vortices and performance of the nozzle.

(2) Chemical reaction

In the present calculations, the fuel is $C_{12}H_{23}$, and the following single step reaction is conducted:

$$C_{12}H_{23} + 17.75O_2 \rightarrow 12CO_2 + 11.5H_2O \quad (2)$$

The finite-rate model is applied to solve the chemical reaction in fuel combustion, in which a single reaction step can be specified to proceed at a finite-rate. This model is restricted to two reactant species. The mass fraction of fuel is calculated by the solution of a transport equation with a source term due to chemical reaction for the finite-rate model. The rate coefficients are assumed to have an Arrhenius form [23]

$$k_f = Ae^{-E/(RT)} \quad (3)$$

where pre-exponential constant $A = 2.9 \times 10^{10}$ kg mol/m^3, activation energy $E/R = 15{,}000$. The rate of reaction is expressed as

$$\omega = k_f[Y_{C_{12}H_{23}}][Y_{O_2}]^{17.5} \quad (4)$$

Table 1 Parameters of chevron mixers

Mixer	Penetration angle α (deg)		
CC	10	20	30
CB	−10	−20	−30
CA	±10	±20	±30

In order to reduce the number of variables to be solved, the mixture fraction method is applied to solve the chemical reaction. Each mixture is tracked with a mixture fraction variable, which is governed by the general transport equation

$$\frac{\partial}{\partial t}(\rho Y_j) + \mathrm{div}(\rho\vec{V}Y_j) = \mathrm{div}(\Gamma^{\varphi}\mathrm{grad}Y_j) + M_j\omega_j + m_j \quad (5)$$

where Y_j is the mass fraction of species i, M_j is the molecular weight, and m_j is the mass generation rate.

Note that this equation contains two source terms: one due to the chemical reaction and the other due to the evaporation of spray droplets. The diffusion coefficient is the same for all mixture fractions. Since the mixture fractions sum to unity (K-1), mixture fraction of the transport equations can be solved when K mixtures are defined. Transport equations for mass fractions of species other than fuel are not solved, but can be calculated from the mixture fractions and the mass fraction of fuel.

(3) Fuel injection

Discrete droplet/particle parcels are tracked through the computational domain by solving the Lagrangian equations. Each parcel represents a number of identical droplet/particles. For steady state calculations, a parcel is tracked through its lifetime (until it evaporates completely).

The momentum equation for the droplet can be written as

$$m_d\frac{d\vec{v}}{dt} = c_D\rho(\vec{V} - \vec{v})|\vec{V} - \vec{v}|\frac{A_d}{2} + m_d g \quad (6)$$

where c_D is drag coefficient, m_d is mass of droplet, $\vec{v}$ is velocity vector of droplet, A_d is the front area of droplet, and g is the gravity.

As the droplet moves through the surrounding medium, it absorbs heat from the mixture and evaporates. For a spherical droplet, the rate of evaporation is modeled as

$$m = 2\pi D_d\rho\Gamma_m \mathrm{Sh}\ln(1 + B_m) \quad (7)$$

where D_d is diameter of droplet and Γ_m represents the diffusion coefficient of the mixture.

The Spalding mass transfer number B_m and Sherwood number are calculated from

$$B_m = \frac{Y_\sigma - Y_i}{1 - Y_\sigma} \quad \mathrm{Sh} = 1 + 0.3\,\mathrm{Re}^{0.5}\,\mathrm{Sc}^{0.333} \quad (8)$$

where Re is the Reynolds number based on the droplet, which is defined as $\mathrm{Re} = \rho D_d|V - v|/\mu_d$ (here, μ is the viscosity), Sc is the Schmidt number (it is 0.8 in this paper), Y_σ is the mass fraction at the droplet surface and it can be calculated from the saturation pressure

$$Y_\sigma = \frac{1}{1 + \left(\frac{p}{p_{sat}} - 1\right)\frac{M}{M_d}} \quad (9)$$

Here, M and M_d represent the molecular weight of the gas and the droplet, respectively.

The mass conservation equation for the droplet can be rewritten in terms of its diameter

$$\frac{d}{dt}D_{\mathrm{d}} = \frac{4\rho\Gamma_{\mathrm{m}}\ln(1+B_{\mathrm{m}})}{\rho_{\mathrm{d}}D_{\mathrm{d}}} \tag{10}$$

The energy equation for the droplet is written as

$$m_{\mathrm{d}}c_{\mathrm{p}}\frac{dT_{\mathrm{d}}}{dt} = \pi D_{\mathrm{d}}^2 q + mQ_{\mathrm{l}} \tag{11}$$

where c_{p} is the specific heat, Q_{l} represents the latent heat, m is the evaporation mass flow rate for each droplet, and q is the heat transfer between the droplet and the surrounding mixture, which can be calculated as [24]

$$q = \frac{2\lambda(T-T_{\mathrm{d}})\mathrm{Nu}\ln(1+B_{\mathrm{m}})}{D_{\mathrm{d}}B_{\mathrm{m}}} \tag{12}$$

where λ is the thermal conductivity of the mixture. The Nusselt number, Nu, is obtained from the following correction [25]:

$$\mathrm{Nu} = 1 + \frac{0.276\mathrm{Re}^{0.5}\,\mathrm{Pr}^{0.333}}{\left(1+\dfrac{1.232}{\mathrm{Re}^{0.5}\,\mathrm{Pr}^{1.333}}\right)^{0.5}} \tag{13}$$

2 Computational Procedure

Due to symmetry in the geometry, it suffices to model a one-quarter sector. In order to apply proper condition at exit, the computational domain is extended downstream of the nozzle to a distance of three times of the nozzle exit diameter in the axial direction and two times in the radial direction.

The boundary conditions required for CFD simulation are the inlet, outlet, solid wall, and symmetry plane conditions. At the inlet, the uniform total pressure and total temperature are specified both core and bypass regions, no consideration of the nonuniformity factor in radial and circumferential directions for simplification, with total pressure 2.25 bar and total temperature 1015 K in the core flow, as well as 2.45 bar and 425 K in the bypass flow. The ratio of the bypass flow to core flow velocity is about 0.32. The core flow is assumed as a gas mixture, having a composition of 70% N_2, 12% CO_2, 14% O_2, and 4% H_2O by mass. The fan flow has a composition of 24.4% O_2 and 75.6% N_2 by mass. The ambient pressure of 0.91 bar is imposed at the outlet. No slip condition and zero-heat flux condition are used on the entire solid wall. Moreover, sector planes are assigned symmetry condition. A turbulence intensity of 1% and a turbulence length scale of 3% of the inlet hydraulic diameter are used.

The injected fuel is assumed to be in the form of droplets of various sizes (Sauter averaged diameter is 40 μm) and these droplets diminish in size in the course of their downstream motion. The fuel inject into the surrounding cells with a random velocity magnitude 20–40 m/s and a random half cone angle of 0–30 deg. The initial conditions for fuel are $T = 330$ K and $P = 7 \times 105$ Pa (for stabilizer). A mixture designated "fuel" may have a composition of 100% $C_{12}H_{23}$.

The multiblock meshes are nonuniform with fine grids in the regions where the complicated flow occurs, especially near the viscous walls. The grid highly refined downstream of the apex of each chevron to minimize the numerical diffusion of the corresponding streamwise vortex. The gird independent tests have performed to decide the mesh numbers. The area-weighted average viscous clustering is employed at all solid walls with a y^+ value less than 30 at all locations, so that the cell closest to the wall can be safely said to be inside the log-law region. In addition, the grid is stretched away from the viscous wall using a stretching ratio less than 1.2. Approximately, two millions computational grids are involved in the completely computational domain.

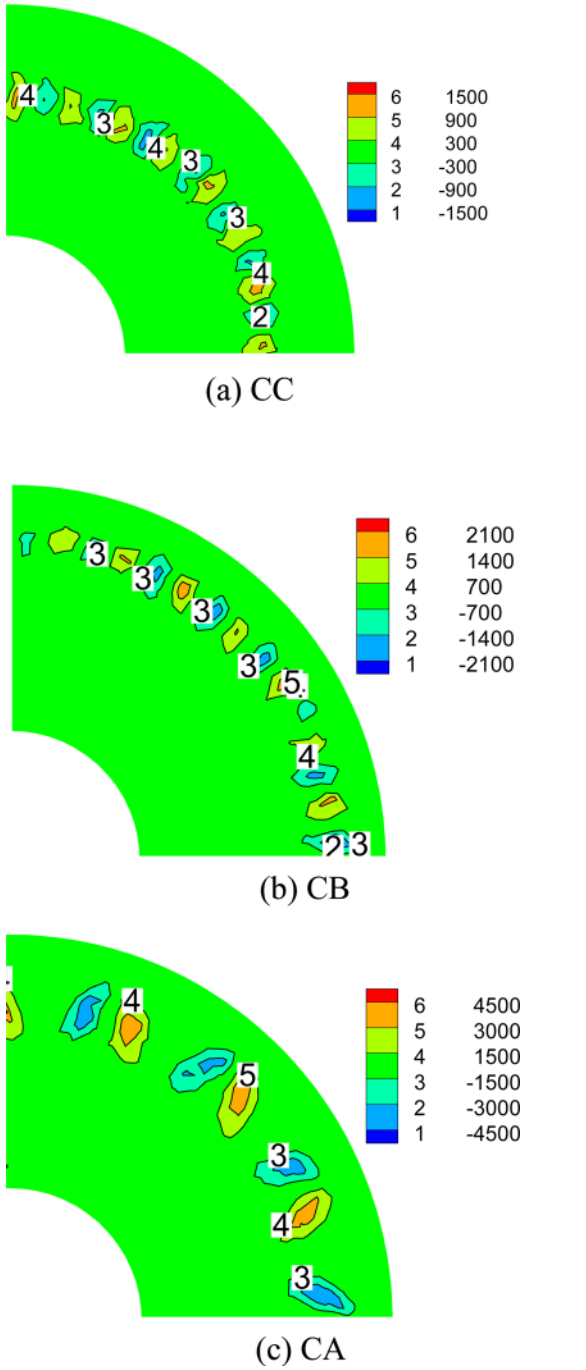

Fig. 5 Streamwise vorticity at mixer exit (unit: s^{-1}): (*a*) CC, (*b*) CB, and (*c*) CA

The three-dimensional numerical simulations have been carried out using the commercial software FLUENT. The coupled solver available in FLUENT has been used with explicit time stepping. All of the calculations have been carried out using second-order-accurate discretization. Convergence is considered achieved when the following criterion has been met: reduction in all residuals of five orders of magnitude. More details on these solvers can be found in the ANSYS FLUENT Software User's Gide [26].

3 Nonreacting Flow Fields

Figure 5 shows the streamwise vortices distributions at the chevron mixer trailing edge section. Here, the chevron penetration angle is set as 20 deg tilted inward either to core flow or to outward to bypass flow.

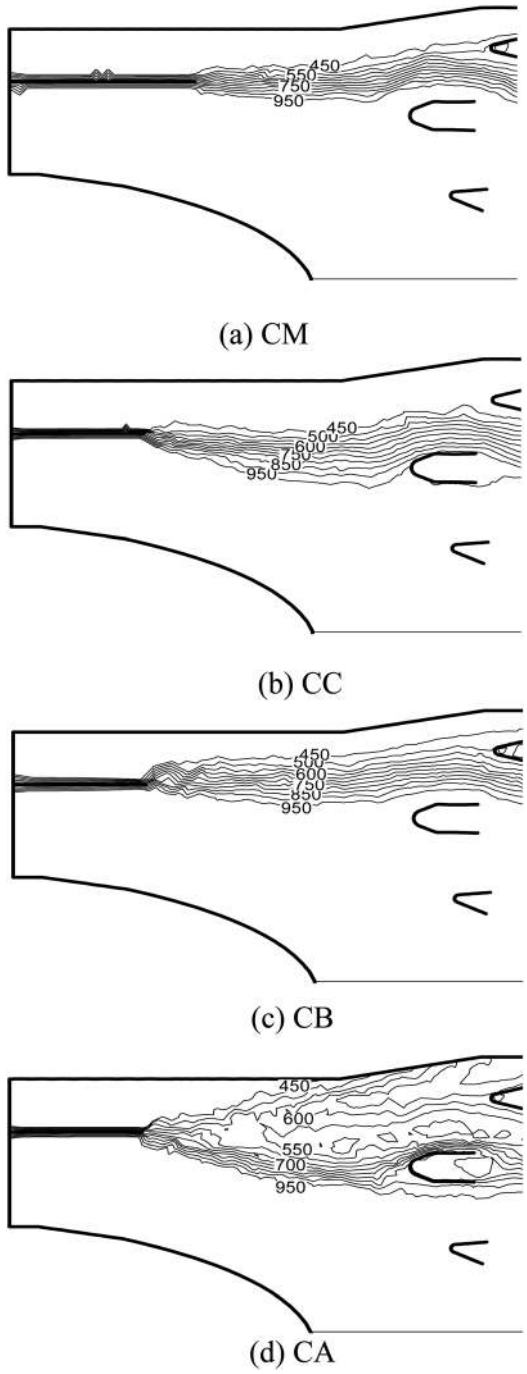

Fig. 6 Local temperature distributions in symmetry plane (unit: K): (*a*) CM, (*b*) CC, (*c*) CB, and (*d*) CA

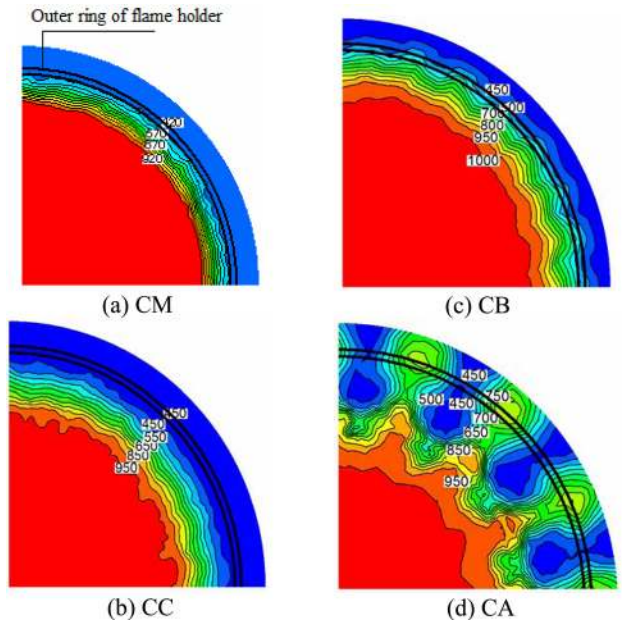

Fig. 7 Temperature distributions at leading edge section of flame holder (unit: K): (*a*) CM, (*b*) CC, (*c*) CB, and (*d*) CA

It is visualized that array pairs of streamwise vortices are shed from chevron mixers, but the vortices number is not double the chevron numbers, meaning that the vortices shedding from adjacent chevrons are merged together in some cases. For CA case, the chevrons incline inward and outward alternately, two vortices induced by adjacent chevrons merge together to form one vortex with wider scale and stronger intensity, which is a benefit to enhance the mixing between core flow and bypass flow.

Figure 6 shows the local temperature distributions for different mixers in the symmetry plane of afterburner. Figure 7 shows the temperature distributions at the leading edge section of flameholder. It is seen that the temperature distribution for the confluent mixer behaves as shear-mixing feature. While for the chevron mixer, the isothermal lines are distorted due to local convective mixing under the action of streamwise vortices shedding from chevrons. For the CC case in which the chevrons are tilted into core flow, the bypass flow is inclined to move inward, leading to an inward distortion of isothermal lines, whereas for the CB case in which the chevrons are tilted into bypass flow, an outward distortion of isothermal lines is seen. By comparison, the distortion is more obvious for CA case in which the chevrons are tilted into core flow and bypass flow alternately, due to the stronger mixing between the core and bypass flows. The mixing enhancement between core flow and bypass flow improves the local temperature distribution at the leading edge section of flameholder for increasing the bypass flow temperature inside afterburner.

In order to evaluate the mixing characteristics quantitatively, the thermal mixing efficiency and total pressure recovery coefficient are defined as [21]

$$\eta = \frac{\int T^{0.5} dm - T_{\mathrm{c}}^{0.5} m_{\mathrm{c}} - T_{\mathrm{b}}^{0.5} m_{\mathrm{b}}}{T_{\mathrm{mix}}^{0.5}(m_{\mathrm{c}} + m_{\mathrm{b}}) - T_{\mathrm{c}}^{0.5} m_{\mathrm{c}} - T_{\mathrm{b}}^{0.5} m_{\mathrm{b}}} \tag{14}$$

$$\sigma = \frac{\int P_{\mathrm{out}}^{*} dm_{\mathrm{out}} / m_{\mathrm{out}}}{\left(\int P_{\mathrm{c}}^{*} dm_{\mathrm{c}} + \int P_{\mathrm{b}}^{*} dm_{\mathrm{b}} \right) / (m_{\mathrm{c}} + m_{\mathrm{b}})} \tag{15}$$

Here, T is the temperature, m is the mass flow rate, T_{mix} is the temperature of fully mixed flow, determined according to $T_{\mathrm{mix}} = (T_{\mathrm{c}} m_{\mathrm{c}} + T_{\mathrm{b}} m_{\mathrm{b}})/(m_{\mathrm{c}} + m_{\mathrm{b}})$ (here, the subscript "c" and "b" denote the core flow and bypass flow, respectively). P^{*} is the total pressure, the subscript "out" means the afterburner outlet section.

The thermal mixing efficiencies for different mixers are shown in Fig. 8. Here, the chevron penetration angle is set as 20 deg tilted inward either to core flow or to outward to bypass flow. The tendencies of thermal mixing efficiency versus mixing length for different mixers are the same in generally. As the mixing length increases, the thermal mixing efficiency is improved gradually. It is noted that the chevron mixers have higher thermal mixing efficiencies in comparison with confluent mixer. Due to the counter-rotating streamwise vortices induced by chevrons, the chevron mixer can increase the mixing efficiency 5–15% in relative to the confluent mixer, which shows the better mixing ability in enhancing the mixing between the core flow and bypass flow. The

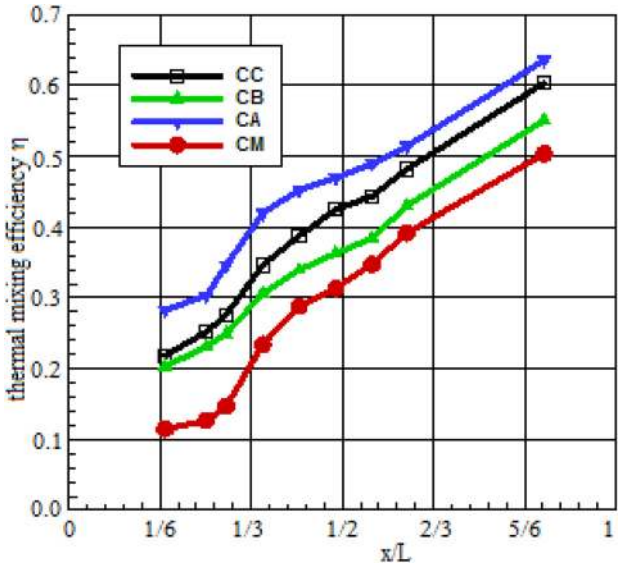

Fig. 8 Thermal mixing efficiencies for various mixers

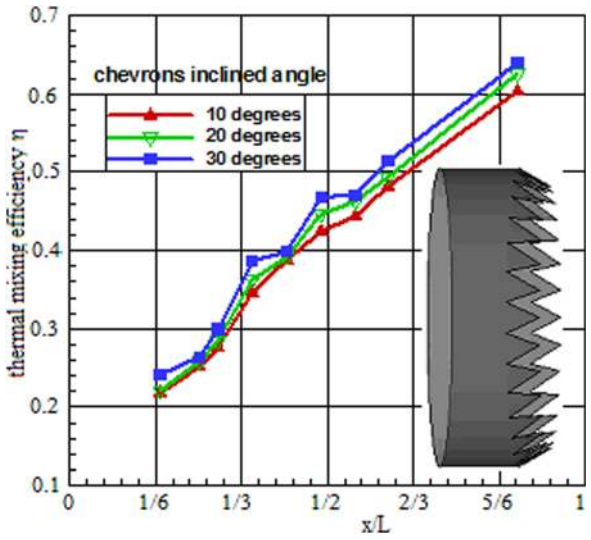

Fig. 9 Effects of chevron titled angle on thermal mixing efficiency in CC case

chevron mixer with chevrons tilted into core flow and bypass flow alternately (CA) demonstrates higher mixing efficiency relative to the other chevron mixers owing to the mixing enhancement.

Figure 9 shows the tilted angle of chevron (CC) on the thermal mixing efficiency. As the chevron inclined angle is increased from 10 deg to 30 deg, the thermal mixing efficiency at axial distance of 2500 mm is increased approximately 9%. It is concluded that the chevrons with bigger tilted angle are contributed to form streamwise vortices with wider scale and stronger intensity.

Figure 10 demonstrates the total pressure recovery coefficient for different mixers. Compared with confluent mixer, the total pressure recovery coefficient of chevron mixer is decreased in a certain extent, especially for higher chevron penetration cases. In general, the total pressure recovery coefficient for the chevron mixer is demonstrated 0.5–1% decrease in comparison with confluent mixer. It is interesting to find that the total pressure recovery coefficient for CA case is higher than the other chevron mixers, although the strongest mixing process between the core and bypass flows occurs in this situation. With the application of chevron mixer inside afterburner, the local flow field is changed downstream of mixer. For CC case in which the chevrons are tilted into core flow, the core flow is forced to distort inward and

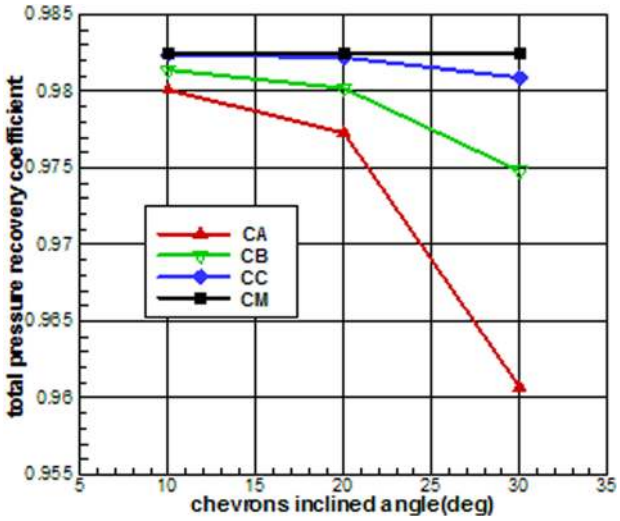

Fig. 10 Total pressure recovery coefficients for various mixers

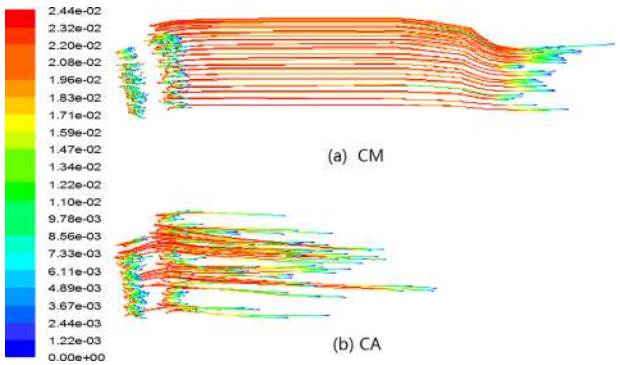

Fig. 11 Fuel droplet diameter distributions at symmetry plane (unit: mm): (*a*) CM and (*b*) CA

impinge the flame holder more seriously. For CB case in which the chevrons are tilted into bypass flow, the bypass flow is forced to distort outward and impinge the augmentor liner more seriously. Whereas for the CA case in which the chevrons are tilted into core flow and bypass flow alternately, the flow distortion inward or outward is enhanced for the stronger mixing between the core and bypass flows, but the flow impingement on the flame holder and augmentor liner is weaken obviously. So that additional flow loss owing to flow distortion and flow impingement on solid wall is relative slight for the CA case. Besides the pressure loss in mixing process, the flow impingement on the flame holder and augmentor liner is most likely to play more important role affecting the overall flow loss inside afterburner. Therefore, the chevrons tilted into core flow and bypass flow alternately take on superiority relative to the other chevron mixers for it could generate stronger streamwise vortices with relatively lower attendant mixing aerodynamic loss inside afterburner. When the chevron inclined angle is increased up to 20 deg, the total pressure recovery coefficient decreases rapidly, mainly due to serious flow impingement on the flame holder and augmentor liner. Therefore, the inclined angle should be designed carefully for the application of chevron mixer inside afterburner.

4 Reacting Flow Fields

The evaporation process of fuel droplets plays an important part in turbulent dissipation and combustion characteristics. Only when the fuel is changed from liquid to vapor, flammable mixture could be ignited with reasonable chemical reaction mechanism. If

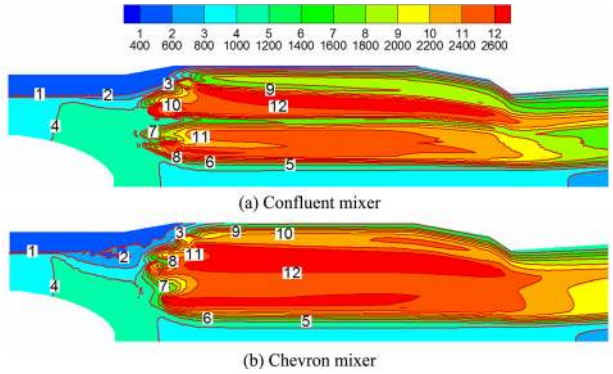

Fig. 12 Temperature distributions of reacting filed at symmetry plane (unit: K): (*a*) confluent mixer and (*b*) chevron mixer

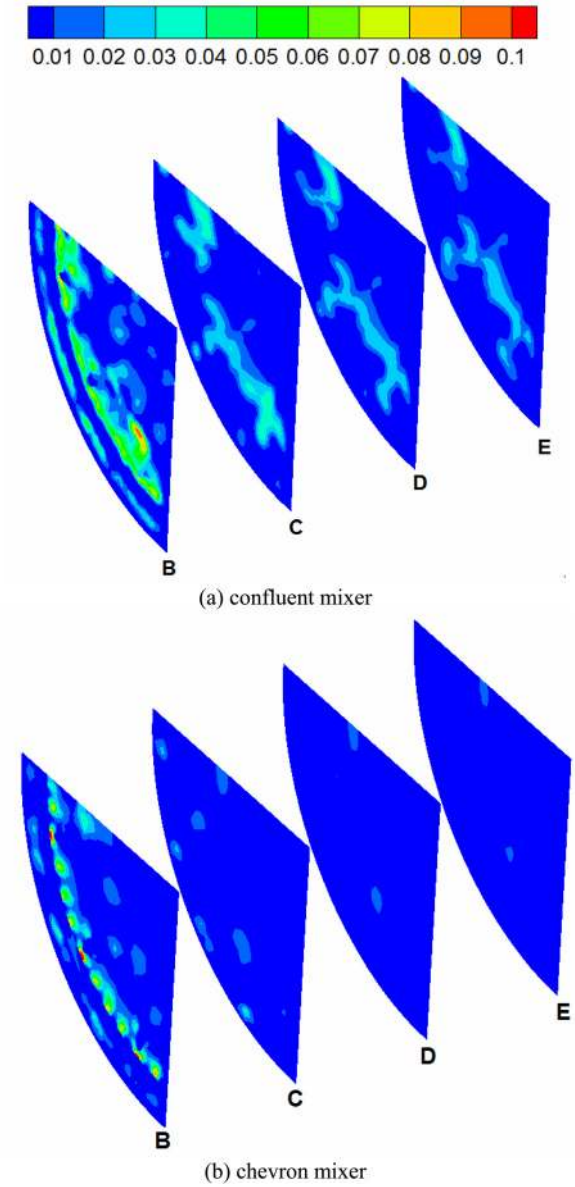

Fig. 13 Fuel mass fraction distributions (the planes defined in Fig. 3(*b*)): (*a*) confluent mixer and (*b*) chevron mixer

fuel could evaporate quickly, the firing process will be going fast and sufficiently, the combustion efficiency will also be enhanced consequently. Figure 11 shows the droplets diameter distributions

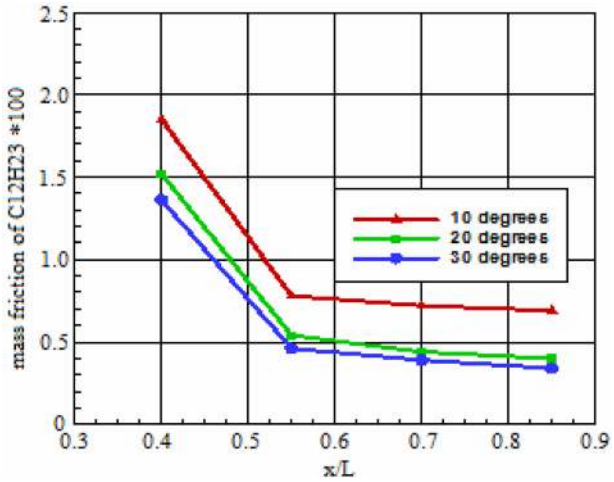

Fig. 14 Sectional area-average fuel mass fraction in CA case (the section defined in Fig. 3(*b*))

Table 2 Combustion efficiencies for several mixers

CM	CA-10 deg	CA-20 deg	CA-30 deg
89.1%	90.8%	91.4%	92.7%

in augmentor of afterburner at the symmetry plane. Here, CA mixer chevrons penetration angle is set as 20 deg.

It can be seen that the lifetime of droplet in bypass region is longer in CM case than that in CA case. Along the streamwise direction, a large amount of fuel droplets is carried by the bypass flow to move downstream for confluent mixer, which will lead to insufficient combustion process. When chevron mixer is employed, fuel droplets injected to the bypass flow evaporated rapidly in short distance with high temperature air heated and stronger forced convection.

Figure 12 shows the temperature distributions inside augmentor at the symmetry plane. The highest temperature reaches 2600 K in both CM case and CA case. It is observed that a high temperature zone is enlarged when the chevron mixer is adopted in contrast to the confluent mixer, due to the stronger heat and mass transfer in convection. Another feature is that a relative "cool zone" appears behind the flameholder in CM case, which is caused by incomplete combustion.

Figure 13 shows the fuel ($C_{12}H_{23}$) mass fraction distributions for different mixers. For convenient presentation in the present paper, five typical sections along the afterburner streamwise direction are labeled from B to E according to priority, as seen in Fig. 3(*b*). It is found that more fuel participates in the chemical reaction for the chevron mixer.

Figure 14 shows the effects of chevron penetration angle on section area-average fuel ($C_{12}H_{23}$) mass fraction distributions along streamwise direction. The average fuel mass fraction decreases rapidly in the front of afterburner, indicating that the chemical reaction rate is more rapid in this region. As chevron penetration angle increases, the chemical reaction rate is enhanced in a certain extent, which is beneficial for improving the combustion efficiency.

Combustion efficiency is defined as follows:

$$\varepsilon = \frac{m_{\text{out}} h^*_{\text{out}} - m_{\text{in}} h^*_{\text{in}} - m_{\text{f}} h_{\text{f}}}{m_{\text{f}} q_{\text{f}}} \tag{16}$$

where the subscript "in" means the afterburner inlet section, h^* is the total enthalpy, m_{f} is the mass of fuel, h_{f} is the enthalpy of fuel, and q_{f} is the heat value of fuel.

Table 2 demonstrates the combustion efficiencies for confluent mixer and chevron mixers. It is observed that the combustion

efficiency for chevron mixer could be increased about 3.5% in comparison with that of confluent mixer. Obviously, better fuel evaporating performance and sufficient combustion process occurred in the afterburner to improve the combustion characteristics when the chevron mixer is utilized.

5 Conclusion

All the results presented in this paper have demonstrated the aerodynamic and mixing characteristics of chevron mixer inside the afterburner of turbofan engine. From all the analysis above, we can conclude that the performances of chevron mixer are superior to confluent mixer.

(1) Due to the counter-rotating streamwise vortices induced by chevrons, the chevron mixer can increase the mixing efficiency 5–15% in relative to the confluent mixer, which shows the better mixing ability in enhancing the mixing between the core flow and bypass flow.
(2) The total pressure recovery coefficient is decreased 0.5–1% compared with confluent mixer. Besides the pressure loss in mixing process, the flow impingement on the flameholder and augmentor liner is most likely to play more important role affecting the overall flow loss inside afterburner.
(3) The chevrons tilted into core flow and bypass flow alternately take on superiority relative to the other chevron mixers as it is of stronger mixing enhancement and lower overall flow loss inside afterburner. The inclined angle should be designed carefully for the application of chevron mixer inside afterburner.
(4) The fuel evaporating performance in the bypass region is improved significantly due to better mixing process, the combustion efficiency for chevron mixer could be increased about 3.5% in comparison with that of confluent mixer.
(5) Although the performance trends of chevron mixer inside an afterburner were predicted by some numerical simulations, the absolute values of the predicted improvements, in particular, require experimental confirmation. The following work would be focused on the optimization of CA chevron parameters as a function of the thermal mixing efficiency and total pressure recovery coefficient.

Acknowledgment

The authors gratefully acknowledge the financial support for this project from the NUAA Fundamental Research Funds, No. NS2013019.

References

[1] Koutmos, P., and McGuirk, J. J., 1989, "Turbofan Forced Mixer/Nozzle Temperature and Flow Field Modeling," Int. J. Heat Mass Transfer, **32**(6), pp. 1141–1153.
[2] Eckerle, W. A., Sheibani, H., and Awad, J., 1992, "Experimental Measurements of Vortex Development Downstream of a Lobed Forced Mixer," ASME J. Eng. Gas Turbine Power, **114**(1), pp. 63–71.
[3] Tsui, Y. Y., and Wu, P. W., 1996, "Investigation of Mixing Flow Structure in Multilobe Mixers," AIAA J., **34**(7), pp. 1386–1391.
[4] O'Sullivan, M. N., Krasnodebski, J. K., Waitz, I. A., Greitzer, E. M., Tan, C. S., and Dawes, W. N., 1996, "Computational Study of Viscous Effects on Lobed Mixer Flow Features and Performance," J. Propul. Power, **12**(3), pp. 449–456.
[5] Yu, S. C. M., and Xu, X. G., 1997, "Turbulent Mixing of Coaxial Nozzle Flows With a Central-Lobed Mixer," J. Propul. Power, **13**(4), pp. 517–524.
[6] Yu, S. C. M., and Xu, X. G., 1998, "Confined Coaxial Nozzle Flow With Central-Lobed Mixer at Different Velocity Ratios," AIAA J., **36**(3), pp. 349–358.
[7] Abolfadl, M. A., Metwally, M. A., El-Messiry, A. M., and Ali, M. A., 2001, "Experimental Investigation of Lobed Mixer Performance," J. Propul. Power, **17**(5), pp. 1109–1116.
[8] Liu, Y., 2007, "Experimental and Numerical Research on High Pumping Performance Mechanism of Lobed Exhauster-Ejector," Int. Commun. Heat Mass Transfer, **34**(2), pp. 197–209.
[9] Shan, Y., and Zhang, J. Z., 2009, "Numerical Investigation of Flow Mixture Enhancement and Infrared Radiation Shield by Lobed Forced Mixer," Appl. Therm. Eng., **29**(17–18), pp. 3687–3695.
[10] Bradbury, L. J. S., and Khadem, A. H., 1975, "The Distortion of a Jet by Tabs," ASME J. Fluid. Mech., **70**(4), pp. 801–813.
[11] Reeder, M. F., and Zaman, K. B. M. Q., 1996, "The Impact of Tab Location Relative to the Nozzle Exit on Jet Distortion," AIAA J., **34**(1), pp. 197–199.
[12] Foss, J. K., and Zaman, K. B. M. Q., 1999, "Large- and Small-Scale Vortical Motions in a Shear Layer Perturbed by Tabs," J. Fluid Mech., **382**, pp. 307–329.
[13] Bridges, J., and Brown, C. A., 2004, "Parametric Testing of Chevrons on Single Flow Hot Jets," AIAA Paper No. 2004-2824.
[14] Callender, B., Gutmark, E., and Martens, S., 2005, "Far-Field Acoustic Investigation Into Chevron Nozzle Mechanisms and Trends," AIAA J., **43**(1), pp. 87–95.
[15] Callender, B., Gutmark, E., and Martens, S., 2008, "Near-Field Investigation of Chevron Nozzle Mechanisms," AIAA J., **46**(1), pp. 36–45.
[16] Behrouzi, P., and McGuirk, J. J., 2006, "Effect of Tab Parameters on Near-Field Jet Plume Development," J. Propul. Power, **22**(3), pp. 576–585.
[17] Rask, O. H., and Gutmark, E., 2007, "Near Field Acoustics of Core and Fan Chevron Nozzles," AIAA Paper No. 2007-437.
[18] Opalski, A. B., Wernet, M. P., and Bridges, J. E., 2005, "Chevron Nozzle Performance Characterization Using Stereoscopic DPIV," AIAA Paper No. 2005-444.
[19] Tide, P. S., and Srinivasan, K., 2009, "Novel Chevron Nozzle Concepts for Jet Noise Reduction," J. Aerosp. Eng. Proc. Inst., Mech. Eng. Part G, **223**(1), pp. 51–67.
[20] Zaman, K. B. M. Q., Bridges, J. E., and Huff, D. L., 2011, "Evolution From 'Tabs' to 'Chevron Technology'—A Review," Int. J. Aeroacoust., **10**(5–6), pp. 685–710.
[21] Yong, S., Jing Zhou, Z., and Liang, X., 2009, "Numerical Investigation of Aerodynamic and Mixing Characteristics of Scarfed Lobed Mixer for Turbofan Engine Exhaust System," Trans. Nanjing Univ. Aeronaut. Astronaut., **26**(2), pp. 130–136.
[22] Yong, S., and Jing-Zhou, Z., 2009, "Numerical Investigation of Flow Mixture Enhancement and Infrared Radiation Shield by Lobed Forced Mixer," Appl. Therm. Eng., **29**(17–18), pp. 3687–3695.
[23] Warnatz, J., Maas, U., and Dibbe, R. W., 1996, "*Combustion, Physical and Chemical Fundamentals, Modeling and Simulation, Experiments, Pollutant Formulation*," Springer-Verlag, Berlin.
[24] Kenneth, K. K., 1986, *Principles of Combustion*, John Wiley Sons, Inc., New York.
[25] Lefebvre, A. H., 1989, *Atomization and Sprays*, Hemisphere Publishing, London.
[26] ANSYS, 2009, ANSYS FLUENT version 12.0, *Software User's Guide*, ANSYS, Inc., Canonsburg, PA.
[27] Koutmos, P., and McGuirk, J. J., 1989, "Turbofan Forced Mixer/Nozzle Temperature and Flow Field Modeling," Int. J. Heat Mass Transfer, **32**(6), pp. 1141–1153.